Biophysical Chemistry 12 (1980) 341–355

FLUORESCENCE DECAY KINETICS OF PYRENE IN MEMBRANE VESICLES

Bang Maw LIU, Herbert C. CHEUNG, Kuang-Ho CHEN [‡] and Mark S. HABERCOM [‡‡]
Biophysics Section, Department of Biomathematics, University of Alabama in Birmingham, Birmingham, Alabama 35294, USA

Received 1 April 1980

The fluorescence decay kinetics of pyrene incorporated into artificial and natural membrane vesicles has been studied by pulse fluorimetry. The emission of monomeric pyrene and its excimer embedded in sonicated liposomes prepared from dipalmitoylphosphatidylcholine and a mixture of this phospholipid and dipalmitoylphosphatidylserine follows a multiple exponential decay law at temperatures both below and above their thermal transitions (10–48°C). When pyrene is incorporated into fragmented skeletal sarcoplasmic reticulum vesicles, the emission decay exhibits similar multiple exponential character. The decay of the monomer in the phospholipid vesicles can be adequately described by three exponential terms. The experimental decays observed with both types of vesicles deviate significantly from a previously proposed model in which departure of the decay of pyrene monomer from monoexponentiality is qualitatively related to a time dependence in the diffusion-controlled formation of excimers from ground state and excited monomers. It is suggested that the observed decays are compatible with a reaction scheme involving excited state interaction.

1. Introduction

Several types of biophysical measurements have been used in recent years to study the properties of biological membranes. Indirect evidence supporting a fluid mosaic membrane structure has been provided by the observation of capping which occurs on lymphocyte surface in the presence of antibodies [1,2] and the finding that newly synthesized lipid molecules readily randomize in fatty acid auxotrophs of *Escherichia coli* cells [3,4]. The capping phenomenon clearly suggests lateral diffusion of membrane bound proteins. More direct evidence for the fluid membrane model has been obtained from the demonstration of lateral diffusion of a variety of paramagnetic derivatives of fatty acids and phospholipids in artificial and natural membranes [5–8]. The technique of fluorescence depolarization has also been widely used to investigate the fluidity of bilayer membranes [9–11], to provide information on phase transition and phase separation in lipsomes and cell membranes [12–15], and to determine rotational mobility of membrane bound proteins [16]. Some of these studies have yielded evidence that many cellular functions are modulated by membrane lipid fluidity.

Since the work of Shinitzky et al. [17] in which the time-averaged (steady state) polarization of a fluorescence probe was used to evaluate the fluidity of the hydrocarbon core of micelles, numerous investigations based on this method have been reported to assess membrane fluidity in a variety of artificial and cell membranes. This assessment is expressed in terms of an apparent "microviscosity" that is obtained through comparison with the polarization of the probe in an isotropic reference medium. Because of the complexity of the bilayer structure and possible anisotropic rotational diffusion and partial immobilization of the probe within the bilayer structure as revealed by nanosecond depolarization measurements, the difficulty in assessing membrane fluidity with a single "microviscosity" value based on steady state measurements has been recently discussed [11,18–20]. In small single-layer vesicles prepared from phospholipids the polarization of the probe diphenylhexatriene does not always tend to zero over the nanosecond time

[‡] Present address: Department of Genetics, Stanford University School of Medicine, Stanford, California 94305, USA.
[‡‡] Present address: Division of Hematology and Oncology, School of Medicine, University of Alabama in Birmingham, University Station, Birmingham, Alabama 35294, USA.

scale even at high temperatures [11,18], indicating that complete randomization of probe motion is not attained. Regardless of the origin of this non-randomization, these findings suggest the need to examine other kinds of hydrophobic membrane probes and to determine through time-resolved measurements other molecular hydrodynamic parameters which may be useful in delineating the complex motions of probe molecules.

A different approach based on fluorescence spectroscopy is through the use of excimer-forming probes. The lateral diffusion of pyrene dispersed in phospholipid vesicles at temperatures above their thermal transitions was first determined by Galla and Sackman [21] from measurements of the monomer and excimer fluorescence intensities and the single excimer lifetime. The method is based on the previous finding that excimer formation in an isotropic medium is diffusion-controlled [22]. Independently, Vanderkooi and coworkers [23,24] described the non-monoexponential decay of pyrene monomer in membranes by a model where excimer formation is assumed to be governed by the general time-dependent diffusion theory of Smoluchowski. By fitting the observed monomer decay data to the model, these workers obtained the lateral diffusion coefficients of pyrene in liposomes above their transition temperatures [24,25] and in red cell ghosts and sarcoplasmic reticulum vesicles [24]. The analysis of the pyrene studies is based on the assumption that the probe molecules are randomized in the bilayer structure. It is intuitively clear that such an assumption may not be valid below the phase transition since phase separation has been demonstrated in phospholipid vesicles, and these authors showed that below the phase transition their results did deviate from the diffusion theories used in their calculations [21,24]. It is not clear whether the bilayer structure above its transition can be safely regarded as both homogeneous and isotropic. The present work was undertaken to examine the monomer and excimer decay of pyrene embedded in artificial and natural vesicles over a temperature range extending from below to above their transitions, and to evaluate how well the emission kinetics can be described by the time-dependent diffusion model. The results which were derived from deconvoluted decay curves indicated that the emission kinetics of either the monomer or excimer confined within the vesicles deviates significantly from the time-dependent diffusion model, regardless whether the temperature is above or below the transition.

2. Materials and methods

2.1. Chemicals

Dipalmitoylphosphatidylcholine (DPPC) and dipalmitoylphosphatidylserine (DPPS) were obtained from Sigma Chemical Co. (St. Louis, MO). Pyrene was obtained from Eastman Organic Chemical Co. (Rochester, NY) and subsequently recrystallized three times from ethanol and water. All other chemicals were of reagent grades.

2.2. Membrane preparations

Single-layer vesicles were prepared from phospholipids which had been dissolved in ethanol/chloroform (1:2 v/v) and dried in a rotary evaporator under reduced pressure. The dried lipid was dissolved at 0.1 mg/ml in 10 mM histidine at pH 7.0 containing 30% sucrose (w/v) and 0.15 M NaCl. The lipid solution was sonicated under nitrogen at 47°C for two hours in a Branson W-40 Sonifier at 80% full power. The sonicated solution was sized by ultracentrifugation at 74 000 g to remove multilamellar vesicles. The supernatant which was shown by electron microscopy to contain single-layer vesicles was used for fluorescence studies with pyrene. Fragmented sarcoplamic reticulum (SR) vesicles were prepared from rabbit by the method of Eletr and Inesi [26]. The purified SR vesicles were suspended at 0°C in a medium containing 30% sucrose (w/v) and 10 mM histidine at pH 7.0. These preparations were shown by polyacrylamide gel electrophoresis in the presence of sodium dodecyl sulfate to be essentially free of contamination [27]. Membrane protein was determined by the method of Lowry et al. [28].

2.3. Fluorimetric measurements

Pyrene was introduced into lipid or SR vesicles by the addition of 1–2 μl of the probe dissolved in hexane to 2 ml of the lipd or SR suspensions under agitation. The lipid suspension was about 0.1 mg/ml and the SR was about 150 μg/ml of protein. Equilibration

was achieved within mixing time. The final pyrene concentration in the suspensions was in the range 1–4 μM. Steady state fluorescence measurements were performed in a ratio spectrofluorimeter previously described [27]. A noncommercial single-photon counting pulse fluorimeter [29] was used to measure fluorescence decay with an air cooled spark gap lamp pulsed at about 50000 Hz. The 336 nm line was selected by a monochromator for excitation. Ditric 3-cavity interference filters were used to isolate the pyrene emission at right angles. Except for measurements at different emission wavelengths, a 370 nm interference filter was used for monomer decay and a 470 nm filter for excimer decay. The fluorimeter was linked to a DEC PDP-8/I minicomputer for data acquisition. Data collection was stopped when the total counts of emitted photons reached about 10^6. A Ludox solution was used to provide a profile of the exciting pulses. Data from the PDP-8/I were transferred by teletype to a Xerox Sigma 7 computer for data analysis.

3. Treatment of nanosecond fluorescence data

3.1. Multiexponential model

Two methods were used to analyze the observed excited state decay curves of pyrene. The first method is based on a nonlinear least squares search [30] for one, two, or three exponentials without regard to the excited state chemistry of the probe. The decay curves were deconvoluted with a computer program which included corrections [31] for non-random errors introduced by sample scattering and zero time shift of the detector system [32]. Three statistical criteria were used to judge the goodness of fit between chosen decay functions and observed data [33]: (1) the reduced chi square ratio, χ^2_R; (2) the autocorrelation function of the residuals; and (3) the weighted residual plot. A chosen decay function was rejected if any one of these criteria was not acceptable.

3.2. Time-dependent diffusion model

The second method is based on the suggestion [24] that the overall emission kinetics of pyrene incorporated into liposomes and biological membranes can be better described by the Smoluchowski diffusion theory in which a time dependence of diffusion is explicitly taken into account. Consider a reaction scheme for excimer formation of pyrene [22,34]:

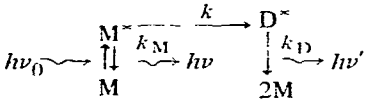

The rate equations governing the time course of the excited monomer and excimer populations are given by [24]

$$dM^*/dt = I_0(1 - 10^{-\epsilon M d}) - k_M M^* - kMM^* , \quad (1)$$

$$dD^*/dt = -k_D D^* + kMM^* , \quad (2)$$

where M^* and D^* are the excited monomer and excimer concentrations, respectively. M is ground state monomer concentration, k_M is the rate constant of excited monomer decay, k_D is the rate constant of excimer decay, and k is the diffusion-controlled bimolecular rate constant for the formation of excimer from ground state monomer and excited monomer [the reciprocals of k_M and k_D are the excited state monomer (τ_M) and excimer (τ_D) lifetimes, respectively]. I_0 is the excitation intensity, ϵ is monomer extinction coefficient, and d is optical path. If the rate constant k is diffusion limited and is independent of time, it is given by $k = 4\pi NRD$, where N is Avogadro's number per millimole, R is twice the reaction radius of monomeric pyrene and D is twice the diffusion coefficient of pyrene. If this rate constant is time-dependent [35], $k = 4\pi NRD\{1 + R/\sqrt{\pi Dt}\}$.

If excitation is effected by a finite impulse, the first term in eq. (1) can be replaced by the excitation pulse, $E(t)$. If a Dirac-δ pulse is used (instantaneous light pulse), the solution of eq. (1) is

$$M^*(t) = M^*(0) \times \exp\{-[k_M + 4\pi NRD(1 + 2R/\sqrt{\pi Dt})M]\,t\}. \quad (3)$$

An equation similar to (but not identical with) eq. (3) was used to analyze the monomer decay of pyrene that was incorporated into lipid vesicles and natural membranes [24].

Since the excitation pulse is always finite, the solution of eq. (1) for this case is

$$M^*(t) = \int_0^t E(u)\,\alpha \exp\{-[A_1(t-u) + A_2(\sqrt{t}-\sqrt{u})]\}\,du\,, \qquad (0 \leq u \leq t)\,, \qquad (4)$$

where α = pre-exponential coefficient, $A_1 = k_M + 4\pi NRDM$, and $A_2 = 8\sqrt{\pi D}NR^2M$. The solution of eq. (2) for the corresponding time course of excimer population is

$$D^*(t) = \int_0^t M^*(u)(B_1 + B_2/\sqrt{u}) \exp[-k_D(t-u)]\,du\,,$$
$$(0 \leq u \leq t, M^*(0) = 0)\,, \qquad (5)$$

where $B_1 = 4\pi NRDM$ and $B_2 = 4\sqrt{\pi D}NR^2M$. Details of this solution are given in Appendix 1. Eqs. (4) and (5) are designated as the three-dimensional time-dependent diffusion model for the emission kinetics of pyrene involving excimer formation. Since in any given set of our lifetime experiments both monomer and excimer decay curves are measured, the time-dependent diffusion model can now be evaluated with all of the experimental data. In the present study when decay curves were modeled by eqs. (3), (4) and (5), the same three statistical criteria used in multiexponential fits were also used to decide how well the observed data were compatible with the time-dependent diffusion model.

Deconvolution calculations of eqs. (4) and (5) can be performed efficiently if a recursion formula is available [31]. For this purpose we have derived a recursion formula and used it in our calculations. This formula is derived in Appendix 2. Examination of eq. (5) shows that $E(t)$ can be replaced by $M^*(t)4\pi NDM(1 + R/\sqrt{\pi Dt})$ in regular deconvolution of lifetime data and $\exp(-t/\tau_D)$ can be used as the fluorescence response function.

Since the motion of a probe constrained within a bilayer may be closer to two-dimensional than to three-dimensional, eqs. (4) and (5) cannot be expected to be strictly valid for the time course of pyrene emission which takes place within small vesicles. A corresponding model of time-dependent diffusion in two-dimensional space was derived by Owen [36] for the decay of monomeric pyrene:

$$M^*(t) = M^*(0) \exp\{-[t/\tau_M + 0.5z\rho D\tau_Q Q(t/\tau_Q)]\}\,, \qquad (6)$$

where τ_M is $1/k_M$, ρ is the density of ground state monomer, τ_Q is a characteristic time equal to R^2/D, z is the longitudinal dimension of the cylinder confining M^* with the radius of this cylinder being the reaction radius of M^*. $Q(t/\tau_Q)$ is given by

$$Q(t/\tau_Q) = \frac{16}{\pi} \int_0^\infty \frac{1 - \exp(-x^2 \cdot t/\tau_Q)}{x^3[J_0^2(x) + Y_0^2(x)]}\,dx\,, \qquad (7)$$

where $J_0(x)$ is the zero order Bessel function of the first kind and $Y_0(x)$ is the zeroth order Bessel function of the second kind. In the cylindrical coordinates used to derive eq. (7) the longitudinal coordinate z (i.e., thickness of the bilayer) is fixed giving a static membtane bilayer. Because of the complexity of the two-dimensional model it is difficult to perform deconvolution on this model. Owen proposed an approximation for $Q(t/\tau_Q)$:

$$Q(t/\tau_Q) = 14.18\sqrt{t/\tau_Q} + 3.17\,t/\tau_Q\,. \qquad (8)$$

Substitution of eq. (8) into eq. (6) yields the following response function

$$M^*(t) = M^*(0) \exp[-(C_1 t + C_2\sqrt{t})]\,, \qquad (9)$$

where $C_1 = k_M + 1.59z\rho D$ and $C_2 = 7.09z\rho R\sqrt{D}$. Since the response function in eq. (9) has the same time dependence as that in eq. (3), it is not necessary to deconvolute eq. (9). Evaluation of the two-dimensional model can be made by comparing the response function, eq. (6), with the response function obtained from the multiexponential fit of the experimental curve.

4. Results

The steady-state emission spectrum of pyrene incorporated into DPPC and DPPC/DPPS vesicles or SR vesicles showed two sharp peaks in the range 370–400 nm with two shoulders on both sides of the long wavelength peak, and a broad peak in the 470 nm region. These spectra are in agreement with those reported for similar systems [24]. The two sharp peaks at 370 and 390 nm have been attributed to monomer emission and the broad peak in the blue region to excimer emission.

The emission kinetics of pyrene incorporated into two types of vesicle was investigated in the temperature range 10–48°C. Three different types of samples were studied: phospholipid vesicles prepared from DPPC, a mixture of DPPC and DPPS (10:1, w/w) and fragmented SR vesicles in the presence of sucrose. The decay curves of both excited monomer and excimer were analyzed by both the multiexponential and time-dependent diffusion models. These results are presented in the following sections.

4.1. Multiexponential fits

The monomer decay in DPPC/DPPS vesicles at 22°C is shown in fig. 1. It cannot be fitted to either a monoexponential or biexponential function (fig. 1a). Although a visual comparison of the observed decay with the chosen biexponential function shown in fig. 1a does not suggest an inadequate fit, the autocorrelation function and weighted residual plots clearly indicate that the chosen function is not compatible with the data. The fitting statistics are considerably improved with a triexponential function as shown in

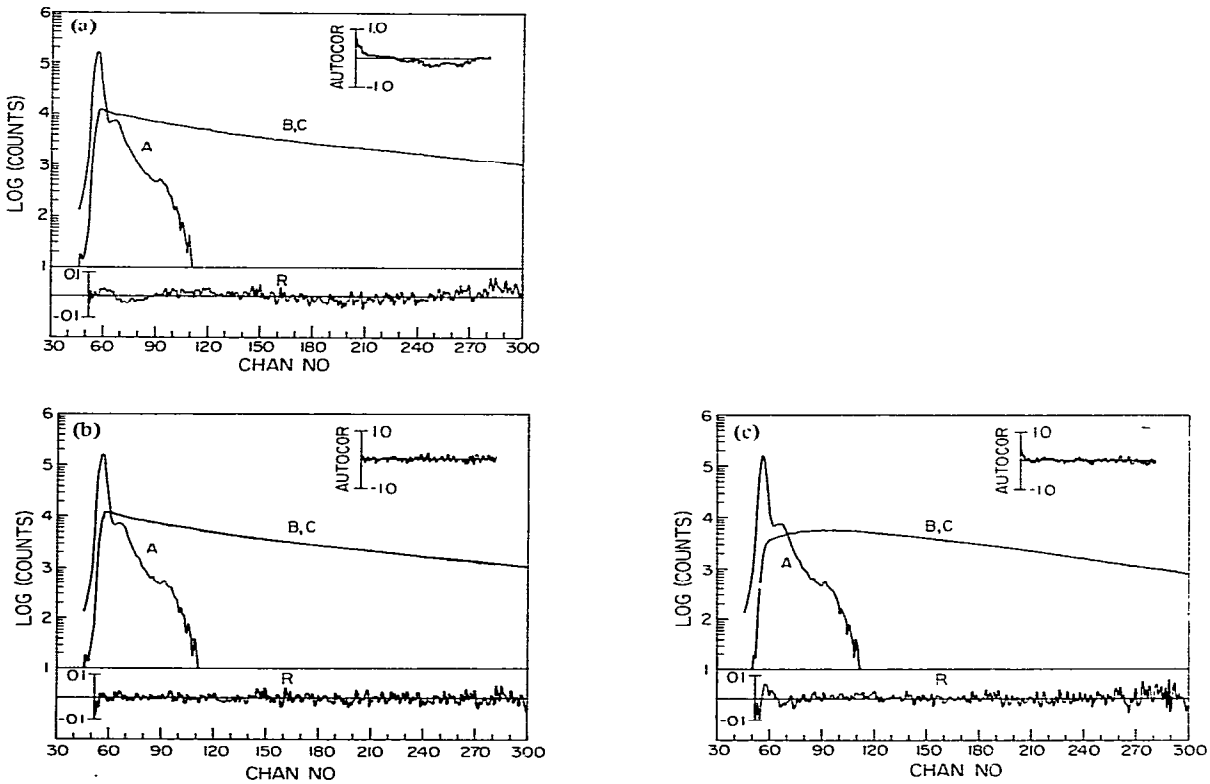

Fig. 1. Fluorescence decay of pyrene in DPPC/DPPS (10:1) vesicles, 22°C. Pyrene concentration was 2.3 μM. Curves A, B, and C are the lamp pulse, experimental curve, and best fitted curve, respectively. Also shown are the autocorrelation function and the weighted residuals (R). (a) Monomer emission decay (at 370 nm) fitted to a biexponential function: $\alpha_1 = 0.43 \pm 0.02$, $\alpha_2 = 0.57 \pm 0.01$, $\tau_1 = 16.9 \pm 1.1$ ns, and $\tau_2 = 96.2 \pm 1.7$ ns; $\chi^2_R = 2.2$. (b) Same set of data as shown in (a) but fitted to a triexponential function: $\alpha_1 = 0.31 \pm 0.03$, $\alpha_2 = 0.35 \pm 0.01$, $\alpha_3 = 0.34 \pm 0.01$, $\tau_1 = 5.2 \pm 0.6$ ns, $\tau_2 = 36.9 \pm 1.3$ ns, and $\tau_3 = 117.8 \pm 1.8$ ns; $\chi^2_R = 1.0$. (c) Excimer emission decay (at 470 nm) fitted to a biexponential function: $\alpha_1 = -0.41 \pm 0.01$, $\alpha_2 = 0.59 \pm 0.01$, $\tau_1 = 25.3 \pm 0.5$ ns, and $\tau_2 = 69.2 \pm 0.5$ ns; $\chi^2_R = 1.5$. Time window: 0.796 ns/channel.

fig. 1b, which yields three lifetimes: $\tau_1 = 5.2$ ns, $\tau_2 = 36.9$ ns, $\tau_3 = 117.8$ ns. The excimer decay of this sample is shown in fig. 1c, where the data are fitted to a biexponential function with acceptable statistics: $\tau_1 = 25.3$ ns, $\tau_2 = 69.2$ ns; $\alpha_1 = -0.41$, and $\alpha_2 = +0.59$. The negative amplitude ($\alpha_1 < 0$) associated with τ_1 reflects formation of excimer immediately after excitation. The subsequent excimer decay (τ_2) with positive amplitude is monoexponential. Equally acceptable multiexponential fits were obtained at 45°C for the decay of both monomer and excimer.

The monomer lifetime data of pyrene in SR vesicles at 22°C are well resolved into two components with $\tau_1 = 25.2$ ns and $\tau_2 = 141.7$ ns, as shown in fig. 2a. When the observed decay is fitted to a triexponential function, no improvement is obtained in the fitting statistics. The corresponding excimer kinetics is well fitted by a biexponential function (fig. 2b) with $\tau_1 = 24.5$ ns, $\tau_2 = 98.2$ ns; $\alpha_1 = -0.47$ and $\alpha_2 = +0.53$. The emission kinetics at 46°C follows the same pattern as that at the lower temperature.

While the decay kinetics of pyrene in phospholipid vesicles is qualitatively different from that in SR vesicles, the results shown in figs. 1 and 2 and those obtained at other temperatures (not shown here) with both samples and with DPPC vesicles demonstrate that the monomer decay can be adequately described by a sum of exponential terms. In contrast, the decay of the excimer appears to be monoexponential in both liposomes and SR vesicles. The best decay parameters derived from these fits are summarized in table 1 for DPPC, DPPC/DPPS, and SR vesicles. While there appears to be a small decrease in the longest lifetime of both monomer and excimer in artificial and SR vesicles with increase in temperature over the narrow range studied, the amplitudes (α_i) of the three monomer lifetimes observed with the DPPC vesicles remain essentially constant. This finding suggests that, if the three lifetimes represent three separate excited species, their proportions are not sensitive to small changes in temperature. However, the observed α_1 and α_2 of monomeric pyrene in SR vesicles show a significant temperature dependence.

4.2. Time-dependent diffusion models

The observed decay curves shown in figs. 1 and 2 are compared with the convolution integrals for three-dimensional time-dependent diffusion. The monomer decay of the probe in DPPC/DPPS at 22°C is fitted to eq. (4) in fig. 3a and the excimer time course is compared with eq. (5) in fig. 3b. A small departure of the observed monomer decay from eq. (4) is indicated in fig. 3a. The departure becomes significant when the chi square ratio ($\chi^2_R = 54$), the autocorrelation function and the weighted residual plots are all considered.

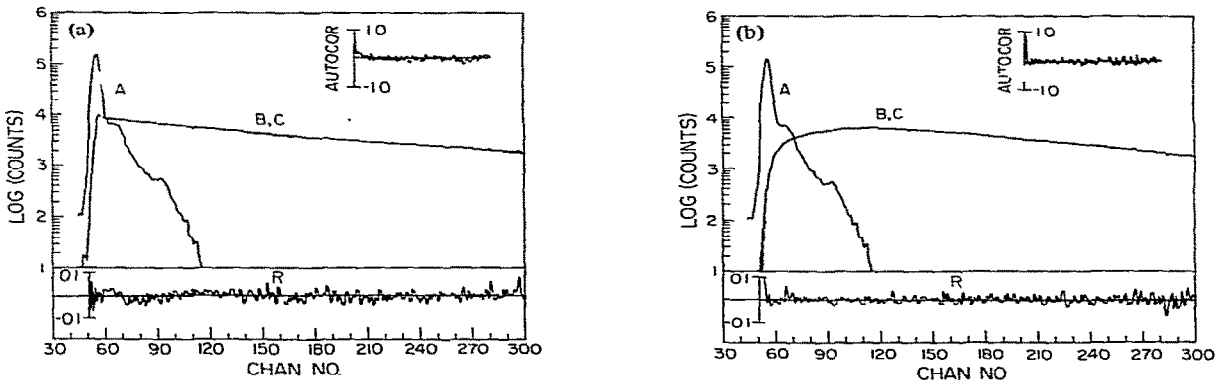

Fig. 2. Fluorescence decay of pyrene in SR vesicles at 22°C. Concentration of pyrene was 4 μM. Curves A, B, and C are the lamp pulse, experimental curve, and best chosen curve, respectively. (a) Monomer decay (370 nm) fitted to a biexponential function: $\alpha_1 = 0.30 \pm 0.01$, $\alpha_2 = 0.70 \pm 0.01$, $\tau_1 = 25.3 \pm 1.7$ ns, $\tau_2 = 141.7 \pm 2.3$ ns; $\chi^2_R = 1.4$. (b) Excimer decay (470 nm) fitted to a biexponential function: $\alpha_1 = -0.47 \pm 0.02$, $\alpha_2 = 0.53 \pm 0.01$, $\tau_1 = 24.5 \pm 0.6$ ns and $\tau_2 = 98.2 \pm 1.2$ ns; $\chi^2_R = 1.0$. Time window: 0.796 ns/channel.

Table 1
Multiple exponential decay of the fluorescence of pyrene in vesicles a), b)

Monomer emission								
Sample	T, °C	α_1	τ_1, ns	α_2	τ_2, ns	α_3	τ_3, ns	χ^2_R
DPPC	22	0.34 ± 0.04	6.5 ± 1.0	0.43 ± 0.04	24.1 ± 2.1	0.23 ± 0.01	118.0 ± 4.5	1.0
	45	0.35 ± 0.05	7.7 ± 1.2	0.45 ± 0.05	23.4 ± 2.3	0.20 ± 0.02	106.8 ± 4.3	1.1
DPPC/DPPS (10:1)	22	0.30 ± 0.04	5.0 ± 0.8	0.34 ± 0.02	35.0 ± 3.3	0.36 ± 0.03	114.9 ± 4.7	1.1
SR	14	0.23 ± 0.02	24.0 ± 3.0	0.87 ± 0.02	152.9 ± 3.2			1.3
	22	0.30 ± 0.03	25.5 ± 2.6	0.70 ± 0.02	141.0 ± 3.6			1.3
	46	0.40 ± 0.01	23.9 ± 0.8	0.60 ± 0.01	132.5 ± 1.7			1.3
Excimer emission								
Sample	T, °C	α_1	τ_1, ns	α_2	τ_2, ns			χ^2_R
DPPC	22	−0.45 ± 0.01	13.1 ± 0.2	0.55 ± 0.01	55.4 ± 3.1			1.8
	45	−0.47 ± 0.01	12.6 ± 0.3	0.53 ± 0.01	35.9 ± 0.2			2.3
DPPC/DPPS (10:1)	22	−0.42 ± 0.02	25.1 ± 0.9	0.58 ± 0.02	69.2 ± 1.0			1.0
SR	14	−0.46 ± 0.01	29.8 ± 0.7	0.54 ± 0.01	115.7 ± 1.6			1.0
	22	−0.44 ± 0.02	24.9 ± 0.6	0.56 ± 0.01	97.6 ± 1.2			1.1
	46	−0.46 ± 0.01	17.3 ± 0.4	0.54 ± 0.01	66.3 ± 0.5			1.0

a) Results averaged from two identical experiments.
b) Transition temperature is 41°C for DPPC and 21–22°C for SR [41].

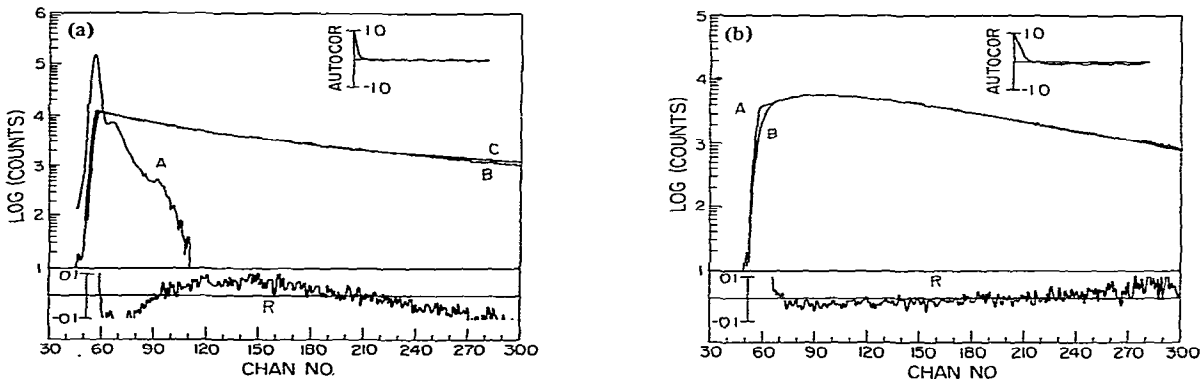

Fig. 3. Fluorescence decay of pyrene in DPPC/DPPS (10:1) vesicles fitted to the three-dimensional time-dependent diffusion model. Same set of data as shown in fig. 1. (a) Monomer decay (370 nm) fitted to eq. (4). Curves A, B, and C are the lamp pulse, experimental curve, and best chosen curve, respectively. Parameters obtained are: $\alpha = 0.027 \pm 0.004$, $A_1 = -(3.6 \pm 0.4) \times 10^6\ s^{-1}$, and $A_2 = (8.8 \pm 0.2) \times 10^6\ s^{-1/2}$; $\chi^2_R = 53.9$. (b) Excimer decay (470 nm) fitted to eq. (5). Curves A and B are the excimer emission curve and best fitted curve, respectively. Parameters are: $\tau_D = 54.0 \pm 0.03$ ns, $B_1 = -(7.1 \pm 0.1) \times 10^6\ s^{-1}$, and $B_2 = (4.72 \pm 0.01) \times 10^6\ s^{-1/2}$; $\chi^2_R = 20.2$. Time window: 0.796 ns/channel.

The best estimates of the two parameters in eq. (4) are $A_1 = -3.6 \times 10^6\ s^{-1}$ and $A_2 = 8.8 \times 10^3\ s^{-1/2}$. Since $A_1 = k_M + (4\pi NRD)M$, a negative value of A_1 would give rise to a negative diffusion coefficient, D, or a negative rate constant k_M for the radiative deactivation of excited monomer. Neither alternative is physically acceptable. Negative values of A_1 were also obtained at other temperatures.

Since we have evaluated the convolution integral for the time course of the excimer population, eq. (5), comparison of the observed excimer emission kinetics with this equation should provide additional information bearing on the time-dependent diffusion model. The comparison in fig. 3b shows that the excimer kinetics is not statistically compatible with eq. (5). The fitted parameters are $B_1 = -7 \times 10^6\ s^{-1}$ and $B_2 = 4.72 \times 10^3\ s^{-1/2}$. The negative value of B_1 is not physically acceptable since $B_1 = (4\pi NRD)M$. This finding is consistent with that derived from monomer data.

The decay curves obtained with SR vesicles cannot be fitted to eqs. (4) and (5) with satisfactory statistics. As with phospholipid vesicles, negative values of A_1 and B_1 are obtained at both high and low temperatures. These results together with those for DPPC vesicles are given in table 2. The high temperature in each case corresponds to that above the known thermal transition of the vesicles and the low temperature to that below the transition. These results indicate that our pyrene decay data obtained from either type of vesicles are not compatible with the Smoluchowski theory of time-dependent diffusion as applied to the emission of pyrene that is confined to small vesicles.

A different way to examine the three-dimensional time-dependent diffusion model is to (1) compute the response function derived from the equation based on the model governing monomer decay, eq. (3), using different values of R, D, τ_M, and M, and (2) compare the computed response function with the response function that is obtained by fitting a given set of experimental decay data to the multiexponential model. Such a comparison is depicted in fig. 4 for DPPC/DPPS at 22°C in which the best triexponential function (from fig. 1b) is shown along with the response function computed for two different total concentrations of pyrene monomer. It appears that the best choice of parameters for eq. (3) would be $\tau_M = 100$ ns, [M] = 100 mM, $R = 10$ Å, and $D = 5 \times 10^{-8}\ cm^2\ s^{-1}$. When the response function derived from this best set of parameters is fitted to the experimental triexponential curve, we obtain an unacceptable χ^2_R (100). A similar conclusion is obtained from the comparison of the best calculated response function with the decay function that is obtained from SR vesicles.

Since the motion of a probe within the bilayer is not isotropic, its diffusion should be confined to a two

Table 2
Fluorescence emission decay parameters of pyrene in membrane vesicles according to the three-dimensional time-dependent diffusion model, eqs. (4) and (5) [a]

Monomer emission				
Sample	T, °C	A_1, $s^{-1/2}$	A_2, $s^{-1/2}$	χ^2_R
DPPC	22	$-(1.00 \pm 0.03) \times 10^7$	$(1.36 \pm 0.02) \times 10^4$	5.8
	45	$-(9.20 \pm 0.20) \times 10^6$	$(1.39 \pm 0.09) \times 10^4$	10.7
SR	14	$-(5.0 \pm 0.7) \times 10^5$	$(4.7 \pm 0.3) \times 10^3$	44.5
	46	$-(4.4 \pm 0.9) \times 10^6$	$(7.9 \pm 0.4) \times 10^3$	85.5

Excimer emission					
Sample	T, °C	B_1, s^{-1}	B_2, $s^{-1/2}$	τ_D, ns	χ^2_R
DPPC	22	$-(1.09 \pm 0.04) \times 10^7$	$(7.2 \pm 0.04) \times 10^3$	39.7 ± 0.5	2.1
	45	$-(2.36 \pm 0.05) \times 10^7$	$(1.1 \pm 0.01) \times 10^4$	30.5 ± 0.4	7.0
SR	14	$-(3.15 \pm 0.25) \times 10^6$	$(4.9 \pm 0.1) \times 10^3$	73.0 ± 1.7	2.5
	46	$-(1.62 \pm 0.07) \times 10^7$	$(1.0 \pm 0.1) \times 10^4$	47.1 ± 1.0	5.4

[a] These are the same sets of data fitted to the multiple exponential model shown in table 1.

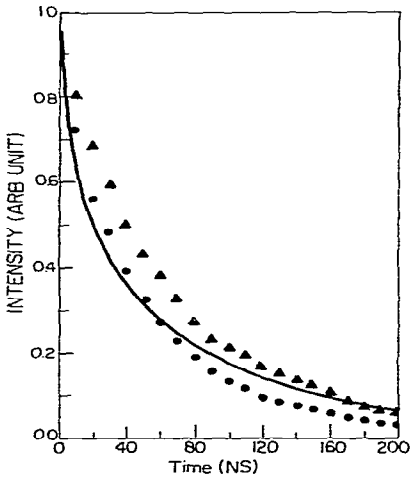

Fig. 4. Comparison of response functions calculated using three-dimensional time-dependent diffusion model, eq. (3), to the multi-exponential decay function of monomer pyrene in DPPC/DPPS (10:1) vesicles, 22°C. The solid curve represents the triexponential decay function [0.31 exp(−t/5.2) + 0.35 exp(−t/36.9) + 0.34 exp(−t/117.8)] obtained from fig. 1b. Response functions calculated from the three-dimensional time-dependent diffusion model, eq. (3), using R = 10 Å, $D = 5 \times 10^{-8}$ cm^2 s^{-1}, and τ_M = 100 ns. (▲): M = 50 mM; (●): M = 100 mM.

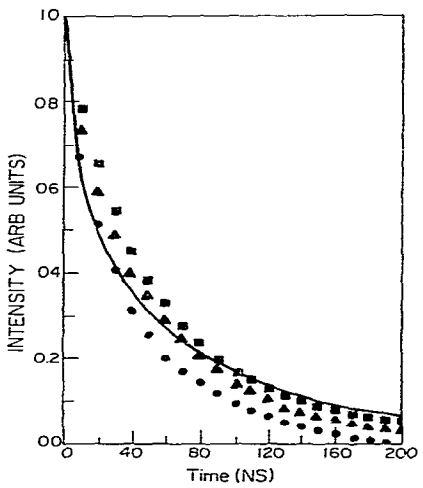

Fig. 5. Comparison of response functions calculated using two-dimensional time-dependent diffusion model, eq. (6), to the multi-exponential decay function of monomer pyrene in DPPC/DPPS (10:1) vesicles, 22°C. The solid curve represents the triexponential decay function shown in fig. 4. Response functions calculated assuming z = 80 Å and R = 10 Å. (▲): $D = 2 \times 10^{-7}$ cm^2 s^{-1}, M = 30 mM, τ_M = 150 ns; (■): $D = 5 \times 10^{-8}$ cm^2 s^{-1}, M = 50 mM, τ_M = 100 ns; (●): $D = 3 \times 10^{-7}$ cm^2 s^{-1}, M = 30 mM, τ_M = 130 ns.

dimensional plane. Eq. (6) which is based on two-dimensional time-dependent diffusion might be more appropriate than the corresponding three-dimensional diffusion model, eq. (3). We present in fig. 5 a comparison of the response function calculated from eq. (6) for different sets of parameters with the experimentally determined triexponential decay from DPPC/DPPS at 22°C. Although the best set of parameters appears to be z = 80 Å, R = 10 Å, τ_M = 150 ns, $D = 2 \times 10^{-7}$ cm^2 s^{-1} and [M] = 30 mM, a large χ^2_R (300) is obtained when the experimental curve is fitted to the best computed function. A similar procedure when applied to the decay data obtained with SR vesicles yields: z = 80 Å, R = 10 Å, τ_M = 100 ns, $D = 10^{-9}$ cm^2 s^{-1}, and [M] = 50 mM. The value of the fitted diffusion coefficient is uncharacteristically too small compared with published lateral diffusion coefficients of small molecules in liposomes and other vesicles [5,37].

4.3. Wavelength dependence of pyrene emission kinetics

Since the non-monoexponentiality of monomeric pyrene emission kinetics cannot be accounted for by either the three-dimensional or two-dimensional time-dependent diffusion model, experiments were performed to obtain information which might suggest alternative physical models. This set of experiments involved analysis of emission decay curves that were obtained at different emission wavelengths. The results indicated that between 370 and 430 nm, the time course was one of decay. In the region 450–480 nm, a growth pattern was observed initially, followed by a decay. Typical response curves obtained at several wavelengths are shown in fig. 6, where they have been normalized with respect to the peak. The peak of emission intensity of the growing species appears approximately 40 ns after excitation. This time scale provides some insight into the kinetics of excimer formation

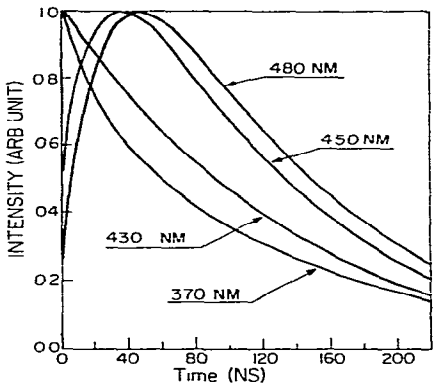

Fig. 6. Fluorescence response functions of pyrene in SR vesicles at different emission wavelengths, 20°C. Concentration of pyrene was 4 μM. Excitation wavelength was 336 nm. The emission wavelength for each response function is indicated.

although the present study was not concerned with this kinetics.

5. Discussion

5.1. Emission kinetics of pyrene in membrane

The decay of excited pyrene embedded in SR vesicles and vesicles obtained from phospholipids can be adequately described by a multiple exponential model. This was demonstrated with monomer and excimer decay data that were obtained at temperatures both above and below the thermal transition of the vesicles. It is generally recognized that multiple-exponential fit by nonlinear least squares is a very difficult problem. It is important to ascertain that convergence to the absolute minimum rather than a local minimum is attained. In all of the reported fits the decay parameters were independent upon initial trial solutions. This finding indicates that the absolute minimum was attained, thus providing an added assurance of the quality of the multi-exponential fits [31].

Several factors could be responsible for the observed fidelity of multiple exponential decays. One is that two or three lipid domains exist in the vesicles giving rise to multiple pyrene sites and that these multiple sites are inherent in the lipid structure, independent of vesicle size. The second possibility is that heterogeneity of pyrene sites is due to molecular packing imposed by the small radius of curvature of the small single-layer vesicles used in our work. This compartmentation of probe is not due to an inherent molecular structure or composition of the bilayer. If the multiple monomer lifetimes indeed reflect heterogeneity of sites (regardless of its origin), the proportion of the sites (α_i) should not be sensitive to temperature variation unless the change is so drastic that individual domains are destroyed. The negligible temperature dependence observed with small phospholipid vesicles suggests probe compartmentation and one of the compartments could arise from the small curvature of the vesicles. This physical constraint may be less severe in SR vesicles since they are generally larger than sonicated lipid vesicles. This could explain the difference in the number of observed lifetimes between the two types of vesicles. It would be tempting to attribute the two monomer lifetimes observed with SR to two lipid domains with one being the phospholipid annulus around the SR ATPase. However, the strong temperature-dependence of the coefficients of the lifetimes argues against this possibility. It is difficult to reconcile the persistence of three pyrene monomer lifetimes observed with liposomes even at temperatures above their thermal transitions. Finally, it is noted that the non-monoexponential decay of pyrene in fluid membrane suspensions became monoexponential when the sample was frozen [24]. These findings support the contention that the observed non-monoexponentiality of monomeric pyrene decay is unlikely to be a result of compartmentation of dispersed pyrene.

There are alternative explanations for non-monoexponential decay behavior. One such alternative is that collision between ground state pyrene with excited pyrene monomer to form excimer is governed by a three-dimensional time-dependent diffusion process, as has been proposed [24]. Birks et al. [22] have given a detailed description of excimer formation in an isotropic medium by assuming the bimolecular rate constant k to be independent of time. Yguerabide et al. [35] have treated theoretically the general process of fluorescence quenching by including a time-dependence for the establishment of a steady state diffusion gradient. The formalism of Yguerabide et al. has been adapted [24] to evaluate the decay of monomeric pyrene embedded in vesicles. In this model, departure of mono-

mer decay from monoexponentiality is attributed to this time-dependent diffusion-controlled process. We tested this mechanisms with the same sets of monomer and excimer decay curves that were well fitted by the multiexponential model. In every case tested, both above and below the transitions of the vesicles, we were unable to obtain satisfactory agreement between our data and the time dependent diffusion model as judged by statistical criteria. In addition, these fits gave rise to either a negative diffusion coefficient or a negative rate constant for monomer decay. We also made a limited test on the corresponding two-dimensional diffusion model and found that our data were also incompatible with the model. These findings differ from those of Vanderkooi and Callis [24]. These authors reported that the decay of monomer in SR at 20°C, in red cell ghosts at 25°C and in egg lecithin and dimyristoyllecithin (DMPC) vesicles above their transition temperatures were better described by the time dependent diffusion model than by a sum of expotential terms. It was also indicated that pyrene in DPPC and DMPC vesicles below their transitions and in mitochondria could not be fitted by the diffusion model. Although reasonable lateral diffusion coefficients were obtained for pyrene in membranes systems where the time-dependent diffusion model was shown by these workers to be valid, it is difficult to judge how well their data were fitted to the model since no fitting statistics were reported. In the present work we also analyzed the excimer decay data and relied on statistical criteria to decide whether an acceptable agreement was obtained between observed decay curves and the diffusion model.

It is not surprising that excimer formation within vesicles at temperatures below the thermal transition does not follow the Smoluchowski theory since phase separation has been demonstrated in such systems [38]. In fact, evidence was obtained by Galla and Sackmann [21] from steady state measurements without invoking the general theory of Smoluchowski that formation of pyrene excimer in DPPC vesicles below its transition was not diffusion-controlled.

The discrepancy between the present results and those published [24] on phospholipid vesicles above the transition temperature and on SR vesicles requires some consideration. Whether an observed decay curve follows a chosen decay law is in general not an easy matter to decide. Usually very accurate and precise data are required to successfully discriminate between alternate models. In addition, the discrimination should be based on established fitting criteria. It is on this basis that the conclusion of the present study are drawn. All decay curves were deconvoluted according to the chosen decay function in spite of the fact that the decay times of pyrene are in general very long compared to the width of the exciting pulse. Deconvolution does not affect the tail portion of the decay curve and may have no detectable effect on the fitted long characteristic time constants, but it certainly affects the initial portion of the decay, particularly the first few nanoseconds. The origin of the time-dependence in the diffusion model arises from the possibility that the spatial distribution of ground state monomer molecules around excited monomer molecules at zero time is not homogeneous. This inhomogeneity may result from a cage effect of neighboring solvent molecules or the anisotropic nature of the bilayer structure. Under this condition there is a finite probability that excimer molecules are formed "instantaneously" in a concentrated pyrene solution immediately upon excitation. The "instanteneous" production of excimer will modify the subsequent diffusion-controlled time course of both excimer and monomer populations. A finite time interval will elapse before a steady state time-independent diffusion gradient can be established [24]. The establishment of this gradient results from readjustment of the initially non-uniform distribution of ground state monomer to a homogeneous distribution. The persistance time of the non-uniform distribution may be very short (< 0.1 ns) in a low viscosity medium at room temperature and its effect may be negligible in so far as the time window of the experiment is concerned. This explains monoexponential decay of pyrene monomer in organic solvents. In a viscous medium or in the interior of a bilayer the non-uniform distribution may persist during a significant fraction of the lifetimes of the excited monomer molecules [35], thus giving rise to a non-monoexponential decay. The non-uniform distribution certainly would be important in the region $t \geqslant 1$ ns. It is in this region of the decay curve where distortion by the finite width of the exciting pulse is the greatest. We do not know how this distortion may affect the fitting of the decay curve to the time-dependent diffusion model, but this possibility should not be discounted.

In the search for an explanation of the present find-

ings that the Smoluchowski theory is not adequate to describe the pyrene emission, it is noted that in the reaction scheme for excimer formation the dissociation of excimer to an excited monomer and a ground state monomer is assumed to be negligible. Its rate constant is not included in the derivation of the rate equations for the monomer and excimer populations. If this step is included in the formulation, the relevant chemical equation to consider would be $M^* + M \underset{k'}{\overset{k}{\rightleftharpoons}} D^* \xrightarrow{k''}$ products. This kinetic scheme clearly requires that the concentration of M^* (or M) decreases initially, followed by a slow growth. Whether the growth portion of the monomer time course is observable will depend upon the magnitudes of k, k' and k''. All decay experiments were carried out to about 240 ns (300 channels) and no indication of a minimum was detected in the monomer time course. It is not clear what effect oxygen quenching may have on the overall emission kinetics since our samples were not degassed prior to measurements. However, it was pointed out [24] that while oxygen did quench the embedded pyrene fluorescence, the calculated diffusion coefficient was independent of oxygen concentration. A third possibility is the fact that free diffusion is assumed in the derivation of eq. (1) for the time-dependent diffusion model. It is possible that fluctuation of the local concentration of embedded pyrene resulting from diffusion might induce an elastic-like compression of the vesivle bilayer [39]. If this deformation is significant, an elastic restoration force which would randomize localized concentration should be included in the formulation.

5.2. Excited state interaction

As an alternate model we suggest that the embedded pyrene undergoes reversible excited state interactions which are not necessarily limited to excimer formation. That reversible excited state interactions can lead to multiple lifetimes has already been indicated [18,40]. Three excited state species, P_1, P_2 and P_3 are assumed as shown in the following scheme.

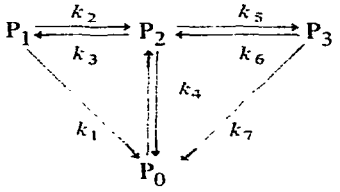

It is further assumed that only P_2 is generated upon excitation of the ground state species P_0 and P_1 and P_3 are formed by transitions of P_2. Each of the three excited species relaxes to ground state by emitting photons with different energies. The following rate equations can be written down:

$$dP_1/dt = -(k_1 + k_2)P_1 + k_3P_2 ,$$

$$dP_2/dt = k_2P_1 - (k_3 + k_4 + k_5)P_2 + k_6P_3 ,$$

$$dP_3/dt = k_5P_2 - (k_6 + k_7)P_3 . \quad (10)$$

Define $x = k_1 + k_2$, $y = k_3 + k_4 + k_5$, and $z = k_6 + k_7$, the characteristic equation with eigenvalue p can be written as

$$\begin{bmatrix} p+x & -k_3 & 0 \\ -k_2 & p+y & -k_6 \\ 0 & -k_5 & p+z \end{bmatrix} \begin{bmatrix} P_1 \\ P_2 \\ P_3 \end{bmatrix} = 0 . \quad (11)$$

In order for this equation to have a nontrivial solution, i.e., where P_1, P_2, and P_3 will not vanish identically, the determinant of the 3 X 3 coefficient matrix in eq. (11) must be equal to zero:

$$P^3 + \alpha_1P^2 + \alpha_2P + \alpha_3 = 0 , \quad (12)$$

where

$$\alpha_1 = \sum_{i=1}^{7} k_i ,$$

$$\alpha_2 = (k_1 + k_7)(k_3 + k_4 + k_5) + k_2(k_4 + k_5 + k_6 + k_7) + k_6(k_1 + k_3 + k_4) + k_1k_7 ,$$

$$\alpha_3 = k_6k_7\{(k_1 + k_2)(k_4 + k_5) + k_1k_3\} - k_5k_6(k_1 + k_2) - k_2k_3(k_6 + k_7) .$$

Assuming that unequal real roots exist for p in eq. (12), the complete solutions for P_1, P_2, and P_3 in the homogeneous eq. (11) will have the following form:

$$P_i(t) = a_i \exp(-t/\tau_1) + b_i \exp(-t/\tau_2) + c_i \exp(-t/\tau_3) \quad (i = 1,2,3) \quad (13)$$

with $-1/\tau_1$, $-1/\tau_2$, and $-1/\tau_3$ being the roots of p in eq. (12). These roots are the negative reciprocals of the

fluorescence lifetime of the three species, $P_1(t)$, $P_2(t)$, and $P_3(t)$. In the absence of additional experimental data, only a qualitative comparison of this model with experimental results is given.

Some qualitative features of this three state model (eq. (13)) are obvious. First, the coefficients a_i, b_i, and c_i depend on initial conditions. For example, $P_1(t)$ and $P_3(t)$ initially are zero; therefore, $a_1 + b_1 + c_1 = 0$ and $a_3 + b_3 + c_3 = 0$. Consequently, at least one of the coefficients for $P_1(t)$ and $P_3(t)$ is negative. This accounts for the appearance of a negative coefficient in the excimer decay function. If the excimer corresponds to $P_1(t)$ and/or $P_3(t)$ and monomer to $P_2(t)$, three lifetimes are obtained as the solution of $P_2(t)$ (eq. (13)). This is in accord with the results of monomer decay obtained from artificial lipid vesicles.

In a rather complex way both the coefficients a_i, b_i, and c_i and the lifetimes τ_1, τ_2, and τ_3 are functions of the rate constants and are highly dependent upon the nature of the medium in which the reactions take place. It is not surprising that only two characteristic times were observed for excimer decay kinetics in all cases studied and for the monomer kinetics in SR. With P_2 assigned to excited monomer, which has a non-zero initial value in the decay function, P_2 may be attributed to the emission in the 370–430 nm region and P_1 or P_3 to the long wavelength emission (450–480 nm). While this assignment does not provide any new information on the energies of the monomer and excimer emission, the formal scheme suggests that the third lifetime observed with phospholipid vesicles can result from a third excited species. The scheme also indicates that the lifetimes of the various species should be resolvable through multiple exponential fits, provided that the various rate constants are favorable for the resolution. At sufficiently low temperatures (i.e., in the frozen state) the formation of one or the other excited species might be considerably slowed down so that the overall monomer decay begins to approach monoexponentiality. This may account for the reported decay behavior observed in the frozen state.

In summary, the present results provide a simple, qualitative model for the fluorescence behavior of pyrene incorporated into vesicles. It is recognized that it may not be possible to discriminate with absolute certainty between alternate models based entirely on kinetic parameters, but in the absence of additional information the simplest of the models should be favored. A more critical evaluation of the present model will require analysis of the decay parameters as a function of pyrene concentration since some of the rate constants should be independent upon this concentration. In addition, spectral evidence for a third species should be sought through measurements of time-resolved emission spectral distribution.

Acknowledgement

This work was supported in part by a grant from the National Institutes of Health (AM-25193).

Appendix I.

Solutions to the equations describing the three-dimensional time-dependent diffusion model, eqs. (1) and (2).

Rewriting eqs. (1) and (2), with the first term replaced by E and k replaced by $4\pi NDRM(1 + R/\sqrt{\pi Dt})$, yields

$$dM^*/dt = E - k_M M^* - 4\pi NDRM(1 + R/\sqrt{\pi Dt})M^* , \quad (A.1)$$

$$dD^*/dt = -k_D D^* + 4\pi NDRM(1 + R/\sqrt{\pi Dt})M^* . \quad (A.2)$$

For convenience, let $A_1 = k_M + 4\pi NDRM$, $A_2 = 8\sqrt{\pi D}NR^2M$, $A'_1 = 4\pi NDRM$, and $A'_2 = 4\sqrt{\pi D}NR^2M$; eqs. (A.1) and (A.2) become

$$dM^*/dt = -(A_1 + A'_2/\sqrt{t})M^* + E , \quad (A.3)$$

$$dD^*/dt = -k_D D^* + (A'_1 + A'_2/\sqrt{t})M^* . \quad (A.4)$$

The integration factor I can be obtained for eq. (A.3)

$$I = \int (A_1 + A'_2/\sqrt{t})\,dt$$

$$= A_1 t + 2A'_2\sqrt{t} = A_1 t + A_2\sqrt{t} . \quad (A.5)$$

Multiplying through eq. (A.3) by $\exp(I)$ and integrating on both sides, one gets

$$M^*(t) = \int_0^t E(u)\exp\{-A_1(t-u) - A_2(\sqrt{t} - \sqrt{u})\}\,du, \quad (A.6)$$

where u is a dummy variable. Similarly the integration factor I' for eq. (A.4) is found to be $k_D t$, and the solution to eq. (A.4) is

$$D^*(t) = \int_0^t (B_1 + B_2/\sqrt{u}) M^*(u) \exp\{-k_D(t-u)\}\, du\,, \tag{A.7}$$

where $B_1 = A_1' = 4\pi NDRM$ and $B_2 = A_2' = 4\sqrt{\pi D} NR^2 M$.

Appendix II.

Recursion formula for pyrene monomer fluorescence decay

The rhs of eq. (A.6) can be replaced by numerical summation in the case of single photon experiment with the channel width = Δt:

$$M^*(i\Delta t) = \sum_{j=0}^{i} \alpha E(j\Delta t) \times \exp[-A_1(i-j)\Delta t - A_2(\sqrt{i\Delta t} - \sqrt{j\Delta t})]\Delta t\,, \tag{A.8}$$

where α is the coefficient and i refers to the ith channel. By the trapezoidal rule, the summation in eq. (A.8) can be written as

$$M^*(i\Delta t) = \tfrac{1}{2}\alpha E(0)\exp(-A_1 i\Delta t)\exp(-A_2\sqrt{i\Delta t})\Delta t + \sum_{j=1}^{i-1} \alpha E(j\Delta t)\exp[-A_1(i-j)\Delta t] \times \exp[-A_2(\sqrt{i\Delta t} - \sqrt{j\Delta t})]\Delta t + \tfrac{1}{2}\alpha E(i\Delta t)\Delta t\,. \tag{A.9}$$

At time $(i+1)\Delta t$, eq. (A.9) gives

$$M^*\{(i+1)\Delta t\} = \tfrac{1}{2}\alpha E(0) \times \exp[-A_1(i+1)\Delta t - A_2\sqrt{(i+1)\Delta t}]\,\Delta t + \sum_{j=1}^{i} \alpha E(j\Delta t)\exp[-A_1(i+1-j)\Delta t] \times \exp\{-A_2[\sqrt{(i+1)\Delta t} - \sqrt{i\Delta t}]\}\Delta t + \tfrac{1}{2}\alpha E\{(i+1)\Delta t\}\Delta t\,. \tag{A.10}$$

The first term on the rhs of eq. (A.10) can be written as

$$\tfrac{1}{2}\alpha E(0)\exp(-A_1 i\Delta t - A_2\sqrt{i\Delta t})\exp(-A_1\Delta t) \times \exp\{-A_2[\sqrt{(i+1)\Delta t} - \sqrt{i\Delta t}]\}\Delta t\,. \tag{A.11}$$

The second term is broken down to two terms:

$$\sum_{j=1}^{i-1} \alpha E(j\Delta t)\exp\{-A_1(i-j)\Delta t - A_2[\sqrt{i\Delta t} - \sqrt{j\Delta t}]\} \times \exp(-A_1\Delta t)\exp\{-A_2[\sqrt{(i+1)\Delta t} - \sqrt{i\Delta t}]\}\Delta t + \alpha E(i\Delta t)\exp(-A_1\Delta t) \times \exp\{-A_2[\sqrt{(i+1)\Delta t} - \sqrt{i\Delta t}]\}\Delta t. \tag{A.12}$$

Therefore, by substituting eqs. (A.9), (A.11), and (A.12) into eq. (A.10), one obtains the recursion relation between $M^*\{(i+1)\Delta t\}$ and $M^*(i\Delta t)$:

$$M^*\{(i+1)\Delta t\} = \{M^*(i\Delta t) + \tfrac{1}{2}\alpha E(i\Delta t)\Delta t\} \times \exp(-A_1\Delta t)\exp\{-A_2[\sqrt{(i+1)\Delta t} - \sqrt{i\Delta t}]\} + \tfrac{1}{2}\alpha E\{(i+1)\Delta t\}\Delta t\,. \tag{A.13}$$

References

[1] L.D. Frye and M. Edidin, J. Cell Sci. 7 (1970) 319.
[2] D.E. Wolf, J. Schlessinger, E.L. Elson, W.W. Webb, R. Blumenthal and P. Henkart, Biochemistry 16 (1977) 3476.
[3] P. Overath, H.U. Schairer and W. Stoffel, Proc. Natl. Acad. Sci. USA 67 (1970) 606.
[4] G. Wilson and C.F. Fox, J. Mol. Biol. 55 (1971) 49.

[5] P. Devaux and H.M. McConnell, J. Am. Chem. Soc. 94 (1972) 4475.
[6] E. Sackmann, H. Träuble, H.J. Galla and P. Overath, Biochemistry 12 (1973) 5360.
[7] M. Petitou, F. Tuy, C. Rosenfeld, Z. Mishal, M. Paintrand, C. Jasnin, G. Mathe and M. Inbar, Proc. Natl. Acad. Sci. USA 75 (1978) 2306.
[8] J.F. Faucon and C. Lussan, Biochim. Biophys. Acta 307 (1973) 459.
[9] U. Cogan, M. Shinitzky, G. Weber and T. Nishida, Biochemistry 12 (1973) 521.
[10] M. Shinitzky and Y. Barenholz, J. Biol. Chem. 249 (1974) 2652.
[11] L.A. Chen, R.E. Dale, S. Roth and L. Brand, J Biol. Chem. 252 (1977) 2163.
[12] C.L. Bashford, C.G. Morgan and G.K. Radda, Biochim. Biophys. Acta 426 (1976) 157.
[13] M. Shinitzky and M. Inbar, Biochim. Biophys. Acta 433 (1976) 133.
[14] M.P. Andrich and J.M. Vanderkooi, Biochemistry 15 (1976) 1257.
[15] R.T. Fraley, D.M. Jameson and S. Kaplan, Biochim. Biophys. Acta 511 (1978) 52.
[16] M. Shinitzky and M. Inbar, J. Mol. Biol. 85 (1974) 603.
[17] M. Shinitzky, A.C. Dianoux, C. Gitler and G. Weber, Biochemistry 10 (1971) 2106.
[18] R. Dale, L.A. Chen and L. Brand, J. Biol. Chem. 252 (1977) 7500.
[19] J.R. Lakowicz and F.G. Prendergast, Science 200 (1978) 1399.
[20] S. Kawato, K. Kinosita, Jr. and A. Ikegami, Biochemistry 16 (1977) 2319.
[21] H.J. Galla and E. Sackmann, Biochim. Biophys. Acta 339 (1974) 103.
[22] J.B. Birks, D.J. Dyson and I.H. Munro, Proc. Roy. Soc. A275 (1963) 575.
[23] J. Vanderkooi, J. Callis and B. Chance, Histochem. J. 6 (1974) 301.
[24] J. Vanderkooi and J. Callis, Biochemistry 13 (1974) 4000.
[25] J. Vanderkooi, S. Fischkoff, M. Andrich, F. Podo and C.S. Owen, J. Chem. Phys. 63 (1975) 3661.
[26] S. Eletr and G. Inesi, Biochim. Biophys. Acta 282 (1972) 174.
[27] M.S. Habercom and H.C. Cheung, Arch. Biochem. Biophys. 191 (1978) 756.
[28] O.H. Lowry, N.J. Rosebrough, A.L. Farr and R.J. Randall, J. Biol. Chem. 193 (1951) 265.
[29] S.C. Harvey and H.C. Cheung, Biochemistry 16 (1977) 5181.
[30] D.W. Marquardt, J. Soc. Indust. Appl. Math. 11 (1963) 431.
[31] A. Grinvald, Anal. Biochem. 75 (1976) 260.
[32] Ph. Wahl, J.C. Auchet and B. Donzel, Rev. Sci. Instr. 45 (1974) 28.
[33] A. Gafni, R.L. Modlin and L. Brand, J. Phys. Chem. 80 (1976) 898.
[34] Th. Foster, Angew. Chem. Internat. Edit. 8 (1969) 333.
[35] J. Yguerabide, M.A. Dillon and M. Burton, J. Chem. Phys. 40 (1964) 3040.
[36] C.S. Owen, J. Chem. Phys. 62 (1975) 3204.
[37] H. Trauble and E. Sackmann, J. Am. Chem. Soc. 94 (1972) 4492.
[38] E.J. Shimshick and H.M. McConnell, Biochemistry 12 (1973) 2351.
[39] W.K. Chan and P.S. Pershan, Biophys. J. 23 (1977) 427.
[40] J.H. Easter, R.P. DeToma and L. Brand, Biophys. J. 16 (1976) 571.
[41] G. Inesi, M. Millman and S. Eletr, J. Mol. Biol. 81 (1973) 483.